Genes & Diseases (2023) 10, 2278–2281

Available online at www.sciencedirect.com

ScienceDirect

journal homepage: www.keaipublishing.com/en/journals/genes-diseases

RAPID COMMUNICATION

m^{6}A regulator-mediated methylation modification patterns and tumor immune microenvironment characterization in endometrial cancer

Endometrial cancer (EC) is the second most prevalent female reproductive system tumor after cervical cancer and its incidence is rising globally.[1] Recently, N6-methyladenosine (m^{6}A) has emerged as an important regulator of a variety of physiological and pathological processes, especially in promoting EC progression.[2,3] However, the potential roles of m^{6}A modification in EC and its immune landscape remain unknown. Here, the correlation between m^{6}A modification patterns and tumor microenvironment (TME) cell-infiltrating characteristics was comprehensively evaluated based on 21 m^{6}A regulators of 1301 endometrial cancer samples. We identified four m6Aclasses characterized by distinct TME cell infiltration. We used principal component analysis algorithms to construct m6Ascore to quantify m^{6}A modification patterns of endometrial cancer individuals. Our results showed that lower m6Ascore may be closely related to immune-inflamed phenotype and displayed immune-activated characteristics and better prognosis, while higher m6Ascore may be associated with immune-desert and immune-excluded phenotype and showed interstitial activation-related characteristics and poor prognosis. These new findings reveal that m^{6}A modification played a nonnegligible role in the formation of TME diversity and complexity and support the possibility of targeting m^{6}A modification patterns for rescuing EC, which were unreported in EC patients.

To clarify this, we integrated the genomic information of EC samples to comprehensively evaluate the m^{6}A modification patterns. The baseline information of all eligible EC datasets was summarized in Table S1. Among the 530 samples, 176 experienced m^{6}A regulators mutations, with a frequency of 33.21% (Fig. S1A). Copy number variation (CNV) was also common among m^{6}A regulators, and most of them focused on CNV amplification, while YTHDF1 and YTHDF2 had extensive CNV deletion frequencies (Fig. S1B). Based on the expression of 21 m^{6}A regulators, we found that the inheritance and expression of m^{6}A regulators between normal and EC samples are highly heterogeneous (Fig. S1B–D). These combined results may account for the unbalanced expression of m^{6}A regulators that played a vital role in the occurrence and progression of EC.

Then we classified patients into four different m^{6}A modification patterns (see the Supplementary Materials and Methods), which were significant differences in m^{6}A regulators transcription profile by unsupervised clustering analysis (Fig. 1A). Prognostic analysis revealed the weaknesses of m6Aclass1 in overall survival and progression-free survival, and the survival strengths of m6Aclass2 and m6Aclass3 (Fig. 1B, C). In order to explore biological behaviors among these four patterns, we conducted gene set variation analysis (GSVA). As shown in Figure S2A and B and Table S4, m6Aclass1 was markedly enriched in stromal activation pathways, m6Aclass2 presented enrichment pathways associated with cell metabolism, and m6Aclass3 was prominently related to the activation of immunity; while m6aclass4 was significantly correlated to cancer biology. Subsequent analysis of TME cell infiltration revealed that all four clusters were enriched in the infiltration of some specific adaptive and innate immune cells (Fig. 1B and Table S3). To our surprise, m6Aclass2 was significantly related to the metabolic pathways such as cell proliferation and metastasis; however, patients with this pattern did not show a matching survival disadvantage (Fig. 1C, D). We found that CD8$^+$ effector T cells were significantly activated by m6Aclass2 (Fig. S2C). Therefore, it was speculated that m6Aclass2 promoted anti-tumor activity by activating immune effector cells. Taken

Peer review under responsibility of Chongqing Medical University.

https://doi.org/10.1016/j.gendis.2023.01.021

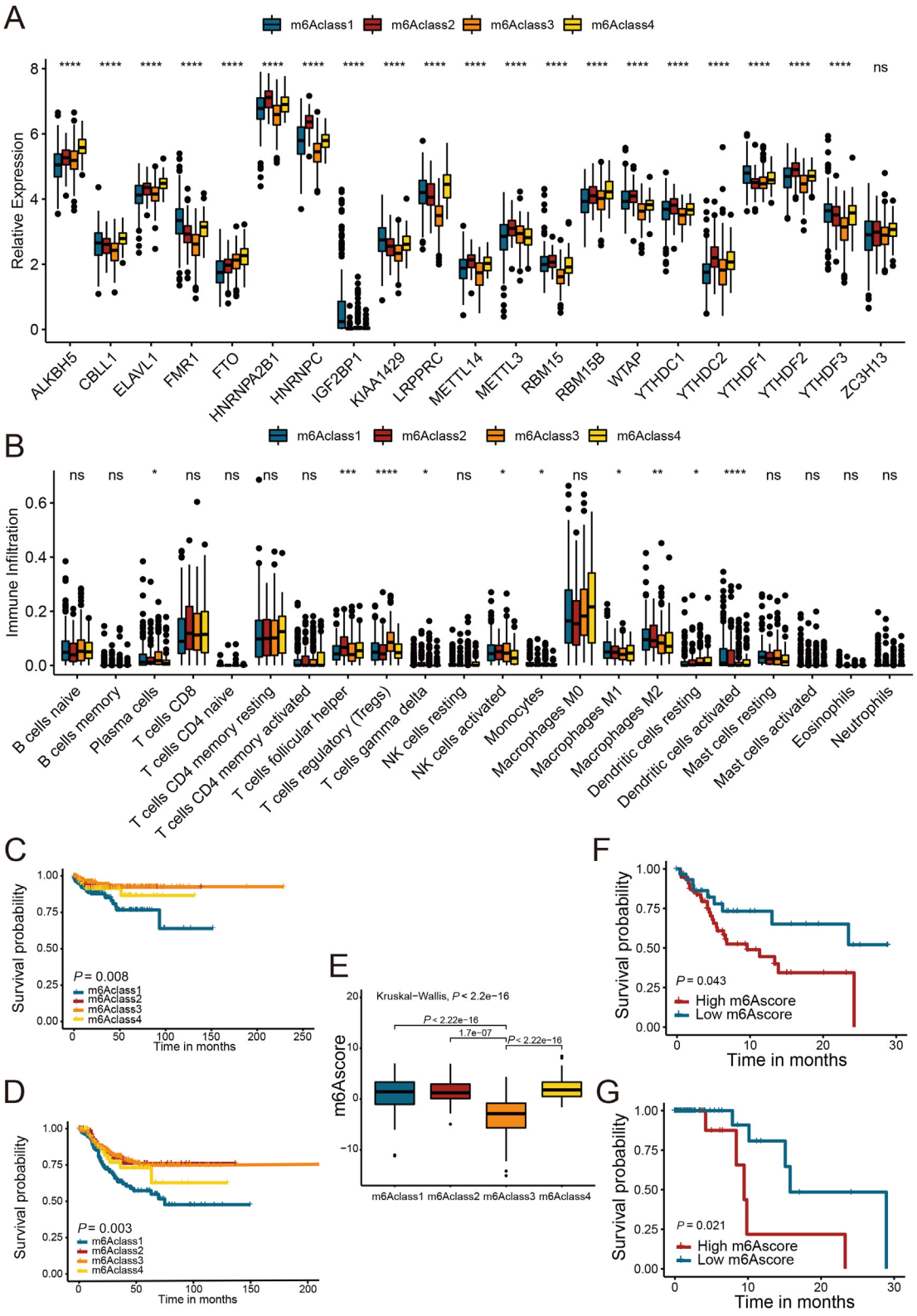

Figure 1 m^{6}A modification patterns, tumor immune microenvironment, and clinical characteristics in endometrial cancer. **(A)** The expression of 21 m^{6}A regulators in the four m6Aclasses. The upper and lower ends of the boxes represented interquartile range of values. The lines in the boxes represented the median value, and the black dots showed outliers. The asterisks represented the statistical *P* values (*$P < 0.05$, **$P < 0.01$, ***$P < 0.001$). **(B)** The abundance of each TME infiltrating cell in four m^{6}A modification patterns. The upper and lower ends of the boxes represented interquartile range of values. The lines in the boxes represented the median value, and the black dots showed outliers. The asterisks represented the statistical *P* values (*$P < 0.05$, **$P < 0.01$, ***$P < 0.001$). Overall survival **(C)** and progression-free survival **(D)** analyses for the four m^{6}A modification patterns based on 657

together, m6Aclass1 was an immune-excluded phenotype, characterized by innate immune cell infiltration and interstitial activation; m6Aclass2 and m6Aclass3 were immune-inflamed phenotypes, characterized by adaptive immune cell infiltration and immune activation; and m6Aclass4 was an immune-desert phenotype, characterized by immunosuppression. Furthermore, we performed spearman correlation analysis to examine the specific correlation between each TME infiltrating cell type and each m^{6}A regulator (Fig. S3A). RBM15, an m^{6}A methyltransferase, was found to be negatively correlated with the infiltration of many TME anti-tumor immune cells. The results indicated that RBM15-mediated m^{6}A methylation may inhibit the activation of TME NK cells and promote the expression of PD-L1, thus weakening the anti-tumor immune response in tumors (Fig. S3B—E).

Next, we identified 3084 differentially expressed genes (DEGs) associated with m^{6}A-related phenotype using limma packages to further study the potential biological processes of each m^{6}A modification pattern. All biological processes significantly associated with the m^{6}A-related phenotype were summarized in Table S6. We conducted an unsupervised cluster analysis based on the above DEGs and divided the patients into four different gene classes which were consistent with the clustering grouping of m^{6}A modification patterns (Fig. S4A—E and Table S5).

Considering the individual heterogeneity and complexity of m^{6}A modification, based on these phenotypically related genes, we constructed a scoring system, named m6Ascore, to quantify the m^{6}A modification patterns of EC individuals (see the Supplementary Materials and Methods). Kruskal—Wallis test indicated that a lower m6Ascore may be closely related to immune-activated characteristics and better prognosis, while a higher m6Ascore may be associated with interstitial activation-related characteristics and poor prognosis (Fig. 1E; Fig. S5A—C). Then, we used the maftools package to analyze the differences in somatic mutation distribution between low and high m6Ascore. As shown in Figure S5D—E, the low m6Ascore group showed a wider burden of tumor mutation than the high group, with the highest mutation rates of 23% and 14% respectively. These results provide a new perspective for exploring the mechanism of m^{6}A methylation modification in EC somatic mutation.

To further explore the characteristics of four m^{6}A modification patterns in different clinical features and biological behaviors, we focused on the TCGA-UCEC and CPTAC-UCEC cohorts. High microsatellite instability (MSI-H) molecular subtypes were characterized by m6Aclass1 and m6Aclass3 methylation patterns, while high CNV_high molecular subtypes were characterized by m6Aclass2 modification patterns (Fig. S6A). We also noted that a higher m6Ascore was significantly associated with MSI and DNA polymerase epsilon (POLE) mutations (Fig. S6B). Compared with the MSI-L subtype, m^{6}A regulators ALKBH5, HNRNPC, RBM15, YTHDC2, and YTHDF2 were significantly up-regulated in the MSI-H subtype while ELAVL1, RBM15, and RBM15B were significantly down-regulated (Fig. S7A). It has been reported that immunotherapy was more effective for tumors with POLE hypermutation and MSI (hot tumors), while it was not effective for tumors with CNV_high and CNV_low (cold tumors). Thus, we inferred that there may be a correlation between m6A modification and immunotherapy. In addition, the tumors modified by the m6Aclass1 methylation pattern were poorly differentiated and enriched in uterine serous carcinoma/uterine papillary serous subtypes (diffuse tissues) (Fig. S7B). In EC, diffuse histological types were significantly associated with poor survival (Fig. S7D). The above results strongly suggested that m6Ascore can better evaluate the subtypes of EC and further evaluate the characteristics of TME cell infiltration and prognosis.

In order to test the stability of the m6Ascore model, we applied the m6Ascore established in EC cohorts and extended it to other reproductive tract cancer cohorts, including cervical squamous cell carcinoma (CESC), ovarian cancer (OV), and prostate adenocarcinoma (PRAD). Our result indicated that m^{6}A modifications were also related to clinical prognosis in other tumors (Fig. S8A—D). Immunotherapy, represented by PD-L1 and PD-1 blocking, has undoubtedly made a major breakthrough in cancer treatment. Based on an immunotherapeutic array, we studied whether m^{6}A methylation modification patterns can predict patients' response to immune checkpoint-blocking therapy. In the anti-PD-1/L1 cohort (GSE176307), patients with low m6Acore had significantly high expression of PD-1, therapeutic advantages, and clinical response against PD-1/L1 immunotherapy, which brought about clinical benefits and prolonged survival time (Fig. S9A—F). In three EC clinical samples, histological types were associated with the expression of 21 m^{6}A regulators and the activity (PD-1) of infiltrated CD8$^+$ T cells and M2 macrophage (Fig. S10). Therefore, the above demonstrated that m^{6}A methylation modification was significantly related to prognosis and the response to anti-PD-1/L1 immunotherapy.

In this work, we discovered an extensive regulation mechanism of m^{6}A methylation modification on TME in EC. This work demonstrated a previously unknown role of m^{6}A methylation modification patterns in the formation of TME diversity and complexity, which will guide us to more effective immunotherapy strategies.

Author contributions

All authors read and approved the final version of the manuscript. Kexin Li participated in conceiving the study, performed most of the computational and statistical analyses, drafted the manuscript, and prepared figures, tables,

patients with endometrial cancer from TCGA-UCEC cohorts including 212 cases in m6Aclass1, 93 cases in m6Aclass2, 272 cases in m6Aclass3, and 80 cases in m6Aclass4. Kaplan—Meier curves with Log-rank *P* values 0.008 **(D)** and 0.003 **(E)** showed a significant survival difference among four m^{6}A modification patterns. The m6Aclass1 showed significantly worse overall survival and progression-free survival than the other three m6Aclasses. **(E)** Differences in m6Ascore among four m6Aclasses in TCGA-UCEC cohort ($P < 0.001$, Kruskal—Wallis test). Survival analyses for low and high m6Ascore patient groups in the **(F)** anti-PD-1 and **(G)** anti-PD-L1 immunotherapy cohort using Kaplan—Meier curves (GSE176307 cohort; $P < 0.05$, Log-rank test).

and supplementary materials. Shanrong Shu drafted the manuscript, participated in conceiving the study, and supervised and coordinated the study. Jiahua Zou discussed the analyses on steps of the study, and critically read and corrected the manuscript. Zhong Liu and Manmei Li received financing, participated in conceiving the study, and supervised and coordinated the study.

Conflict of interests

The authors declare no conflict of interests.

Funding

This work was supported by the National Natural Science Foundation of China (No. 82073864, 82073895) granted to Zhong Liu, the Science and Technology Planning Project of Guangzhou, China (No. 202002030294, 202102010134), the Basic and Applied Basic Research Foundation of Guangdong, China (No. 2021A1515220126, 2018B030311020) granted to Manmei Li and Shanrong Shu.

Appendix A. Supplementary data

Supplementary data to this article can be found online at https://doi.org/10.1016/j.gendis.2023.01.021.

References

1. Clarke MA, Long BJ, Del Mar Morillo A, et al. Association of endometrial cancer risk with postmenopausal bleeding in women: a systematic review and meta-analysis. *JAMA Intern Med*. 2018;178(9):1210—1222.
2. Zhang L, Wan Y, Zhang Z, et al. IGF_2BP_1 overexpression stabilizes PEG10 mRNA in an m6A-dependent manner and promotes endometrial cancer progression. *Theranostics*. 2021;11(3):1100—1114.
3. Liu J, Eckert MA, Harada BT, et al. m^6A mRNA methylation regulates AKT activity to promote the proliferation and tumorigenicity of endometrial cancer. *Nat Cell Biol*. 2018;20(9):1074—1083.

Kexin Li [a], Shanrong Shu [b,**], Jiahua Zou [a], Manmei Li [c,***], Zhong Liu [a,*]

[a] *Guangdong Provincial Key Laboratory of Bioengineering Medicine, National Engineering Research Center of Genetic Medicine, Institute of Biomedicine, College of Life Science and Technology, Jinan University, Guangzhou, Guangdong 510632, China*
[b] *Department of Gynecology and Obstetrics, The First Affiliated Hospital of Jinan University, Guangzhou, Guangdong 510630, China*
[c] *International Cooperative Laboratory of Traditional Chinese Medicine Modernization and Innovative Drug Development of Chinese Ministry of Education (MOE), School of Pharmacy, Jinan University, Guangzhou, Guangdong 510632, China*

*Corresponding author.

**Corresponding author.

***Corresponding author.
E-mail address: tliuzh@jnu.edu.cn (Z. Liu)

10 August 2022
Available online 24 March 2023